Threshold Profiling for Wideband Ranging

Stefania Bartoletti, *Member, IEEE*, Andrea Conti, *Senior Member, IEEE*, Wenhan Dai, *Student Member, IEEE*, and Moe Z. Win, *Fellow, IEEE*

***Abstract*—This letter establishes a methodology to design threshold profiles for wideband ranging systems. Differently from conventional methods using a single threshold value that is designed based on the signal detection and false-alarm probability requirements, we propose a threshold profile that is designed based also on the ranging error requirement. The proposed method relies only on channel statistics without requiring channel estimation. A case study shows that, compared to conventional methods, the proposed method for threshold profiling significantly improves the performance in terms of false-alarm probability, detection probability, and ranging error.**

***Index Terms*—Wideband ranging, time-of-arrival estimation, energy detection, threshold profiling.**

I. Introduction

NETWORK LOCALIZATION [1] is a key enabler for a variety of emerging applications including autonomous vehicles, smart cities, logistics, public safety, environmental monitoring, and social networks [2]–[10]. Range-based network localization relies on measurements of distances between wireless nodes [11]–[13]. In particular, ranging techniques based on time-of-arrival (TOA) estimation are widely adopted, especially for high-accuracy wideband localization in harsh propagation environments (e.g., indoor). Conventional techniques for TOA estimation rely on threshold-based detection, in which the choice of the threshold is crucial for detection probability, false-alarm probability, and ranging error.

The design of threshold-based detectors is challenging due to impairments in wireless channels such as multipath, obstructions, and noise. If the knowledge of the instantaneous channel (multipath amplitudes and delays) is available, then the matched filter enables the optimal coherent detection [11]. However, non-coherent detectors, which require only the knowledge of channel statistics (power decay and noise floor), are preferred to coherent detectors for their lower complexity.

A popular non-coherent detector is the energy detector (ED), which determines the TOA by comparing energy samples collected in consecutive dwell intervals with a threshold [14]–[17]. In conventional approaches, the threshold is the same for all dwell intervals and is chosen to provide a constant false-alarm rate (CFAR) [18]. Specifically, the threshold is determined by accounting only for the noise without considering the wireless environment [19]–[22]. Accounting for the wireless environment would result in a threshold profile (i.e., a different threshold for each dwell interval) instead of a threshold value. For example, a delay-dependent threshold was obtained via simulation in [23].

This letter proposes a method for designing threshold profiles for wideband ranging systems. The proposed threshold profile meets the requirements on ranging error in addition to those on false-alarm probability and detection probability. In particular, a tractable expression for the threshold profile is derived for wideband signals. The performance improvement of threshold profiling with respect to fixed thresholds is quantified in a case of study.

Manuscript submitted September 7, 2017; revised December 26, 2017.

S. Bartoletti and A. Conti are with the Department of Engineering and CNIT, University of Ferrara, 44122 Ferrara, Italy (e-mail: stefania.bartoletti@unife.it; a.conti@ieee.org).

W. Dai and M. Z. Win are with the Laboratory for Information and Decision Systems, Massachusetts Institute of Technology, Cambridge, MA 02139, USA (e-mail: whdai@mit.edu; moewin@mit.edu).

This research was supported, in part, by the European Union's Horizon 2020 research and innovation programme under the Marie Skłodowska-Curie Grant 703893, the Office of Naval Research under Grants N62909-18-1-2017 and N00014-16-1-2141, and the Copernicus Fellowship.

Digital Object Identifier XX.YYYYY/LSP.2018.ZZZZZZZ

II. Ranging System Model

This section presents the ranging system model: first, the statistical distribution of the energy samples is provided; and then, the range inference method is described.

A. Energy Samples

Consider a transmitter at position $\boldsymbol{p}_{\mathrm{t}}$ and a receiver at position $\boldsymbol{p}_{\mathrm{r}}$. The transmitter emits a sequence containing N_{sr} replicas of a signal $s(t)$, with repetition frequency $f_{\mathrm{sr}} = 1/T_{\mathrm{sr}}$, which are non-coherently accumulated at the receiver. At the receiver, the replicas are non-coherently accumulated. The aim of a ranging system is to detect the presence of the signal $s(t)$ from the received waveform and to estimate its TOA τ with respect to a reference time t_0.[1] The reference time t_0 can be the time at which the signal was transmitted (e.g., localization or radar networks based on TOA) or be the time shared among several receivers (e.g., localization or radar networks based on time-difference-of-arrival).

Fig. 1 illustrates the signal processing elements for an ED-based ranging system after band-pass filtering for noise reduction (and after clutter mitigation in radar networks).[2] In particular, the filtered signal $r(t)$ is first sampled by an analog-to-digital converter (A/D) with sampling interval T_{s}. The waveform samples are then processed by a quadrature integrate and dump (QID) block that squares and integrates the samples over a dwell time T_{d} to obtain $N_{\mathrm{bin}} = \lfloor T_{\mathrm{obs}}/T_{\mathrm{d}} \rfloor$ energy bins within the observation time T_{obs}, where $\lfloor x \rfloor$ is the greatest integer less than or equal to x. Each bin is obtained from $N_{\mathrm{sb}} = \lfloor T_{\mathrm{d}}/T_{\mathrm{s}} \rfloor$ received samples. The ith bin corresponds to the integration interval $\mathcal{T}_i = (T_{\mathrm{d}}\, i, T_{\mathrm{d}}\, (i+1)]$

[1] Range and TOA are used interchangeably throughout this letter since the former is a bijective function of the latter.

[2] Note that the results of this paper can be applied also to different versions of ED-based ranging systems (e.g., [24]).

This article has been accepted for publication in a future issue of this journal, but has not been fully edited. Content may change prior to final publication. Citation information: DOI 10.1109/LSP.2018.2815692, IEEE Signal Processing Letters

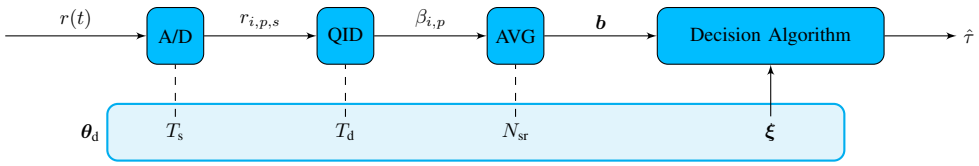

Fig. 1. Ranging system based on energy detection.

with $i \in \mathcal{B} = \{0, 1, \ldots, N_{\mathrm{bin}} - 1\}$. The energy bins are then processed by an averaging (AVG) block over the N_{sr} replicas to increase the signal-to-noise ratio (SNR). The output of the AVG block results in a vector of energy bins $\boldsymbol{b} = [\, b_0, b_1, \ldots, b_{N_{\mathrm{bin}}-1} \,]$. A ranging algorithm chooses a bin index $\hat{\imath}$ based on the energy bin vector $\boldsymbol{b}$. The TOA estimate is then determined as a value inside the interval $\mathcal{T}_{\hat{\imath}}$ according to a function $\hat{\tau} = g(\hat{\imath})$ (e.g., $g(\hat{\imath}) = \hat{\imath} T_{\mathrm{d}} + T_{\mathrm{d}}/2$).

Each element b_i of $\boldsymbol{b}$ is the instantiation of a random variable (RV) b_i with probability distribution depending on the transmitted signal, the true TOA τ, the wireless channel, and the ED parameters. Let $\boldsymbol{\theta}_{\mathrm{b}} = [\tau, \boldsymbol{\theta}_{\mathrm{h}}, \boldsymbol{\theta}_{\mathrm{d}}]$ denote the parameter vector, with $\boldsymbol{\theta}_{\mathrm{h}}$ representing the wireless channel parameters (including the amplitude and arrival time of multipath components) and $\boldsymbol{\theta}_{\mathrm{d}}$ representing the ED parameters (including dwell time and threshold values). The normalized bin values $\mathsf{b}_i N_{\mathrm{sr}}/\sigma^2$, with $i \in \mathcal{B}$, conditioned on $\boldsymbol{\theta}_{\mathrm{b}}$ are independent and distributed as noncentral chi-squared RVs with $N_{\mathrm{sr}} N_{\mathrm{sb}}$ degrees of freedom [14], i.e.,

$$\mathsf{b}_i \frac{N_{\mathrm{sr}}}{\sigma^2} \overset{|\boldsymbol{\theta}_{\mathrm{b}}}{\sim} \chi^2_{N_{\mathrm{sr}} N_{\mathrm{sb}}}(\lambda_i)\,. \tag{1}$$

The parameter λ_i is the non-centrality parameter that depends on $\boldsymbol{\theta}_{\mathrm{b}}$ and is given by

$$\lambda_i = \sum_{p=0}^{N_{\mathrm{sr}}-1} \sum_{s=0}^{N_{\mathrm{sb}}-1} \frac{u^2_{i,p,s}}{\sigma^2} \tag{2}$$

where $u_{i,p,s} = u\,(t_{i,p,s})$ is the sample of the signal after propagating through a wireless channel with impulse response $h(t)$; $t_{i,p,s} = i\,T_{\mathrm{d}} + p\,T_{\mathrm{sr}} + s\,T_{\mathrm{s}}$ is the sampling instant; and σ^2 is the variance of the zero-mean Gaussian noise.

B. Range Inference

Several TOA estimation algorithms can be found in the literature when the input is a vector of energy bins, including the threshold crossing search (TCS), jump back and search forward (JBSF), and serial backward search (SBS) [11]. Most of them require the comparison of each bin value with a threshold. In the following, the TCS algorithm is used as a case study to illustrate the design of the threshold profile; a similar approach can be used for other threshold-based algorithms.

The TCS algorithm first searches for any bin value b_i that crosses a threshold ξ_i for all $i \in \mathcal{B}$. The algorithm then selects, if $\mathcal{C}_{\mathrm{th}} = \{\exists i \in \mathcal{B} \text{ s.t. } \mathsf{b}_i > \xi_i\}$ occurs, the bin index $\hat{\imath}$ as the smallest i for which $\mathsf{b}_i > \xi_i$. When $\mathcal{C}_{\mathrm{th}}$ does not occur, the signal is undetected and the TOA is not estimated [25].

Consider the parameter vector $\boldsymbol{\theta}$ such that the corresponding $\boldsymbol{\lambda} \neq \mathbf{0}$, where $\boldsymbol{\lambda} = [\lambda_0, \lambda_1, \ldots, \lambda_{N_{\mathrm{bin}}-1}]$ is the vector of non-centrality parameters. The detection probability is given by

$$P_{\mathrm{d}}(\boldsymbol{\theta}_{\mathrm{b}}) = 1 - \prod_{i \in \mathcal{B}} F_{\mathsf{b}_i}(\xi_i | \boldsymbol{\theta}_{\mathrm{b}}) \tag{3}$$

where $F_{\mathsf{b}_i}(\cdot|\boldsymbol{\theta}_{\mathrm{b}})$ is the cumulative distribution function (CDF) of the RV b_i that depends on the parameter vector $\boldsymbol{\theta}_{\mathrm{b}}$. The false-alarm event occurs when, in the absence of the transmitted signal, the signal is incorrectly detected.[3] Consider the parameters vector $\boldsymbol{\theta}$ such that the corresponding $\boldsymbol{\lambda} = \mathbf{0}$. The false-alarm probability is given by

$$P_{\mathrm{fa}}(\boldsymbol{\theta}_{\mathrm{b}}) = 1 - \prod_{i \in \mathcal{B}} F_{\mathsf{b}_i}(\xi_i | \boldsymbol{\theta}_{\mathrm{b}})\,. \tag{4}$$

The ranging error can be characterized in several ways. For a true TOA $\tau \in \mathcal{T}_i$, the minimum ranging error is obtained when the bin $i = \lfloor \tau / T_{\mathrm{d}} \rfloor$ is selected, for which $|\hat{\tau} - \tau| \leqslant T_{\mathrm{d}}$ for any $g(\cdot)$. Considering the parameters vector $\boldsymbol{\theta}$ for $\tau \in \mathcal{T}_i$, the probability of selecting the correct bin i is

$$P_{\mathrm{c},i}(\boldsymbol{\theta}_{\mathrm{b}}) = \Big[1 - F_{\mathsf{b}_i}(\xi_i | \boldsymbol{\theta}_{\mathrm{b}})\Big] \prod_{j \in \mathcal{I}_i(i)} F_{\mathsf{b}_j}(\xi_j | \boldsymbol{\theta}_{\mathrm{b}}) \tag{5}$$

where $\mathcal{I}_n(m) \triangleq \mathcal{B} \cap \{m - n, m - n + 1, \ldots, m - 1\}$, with $m > n$ and $m > 0$, and is empty for $n \leq 0$.

III. Design of Threshold Profile

The design of the threshold profile vector $\boldsymbol{\xi} = [\xi_0, \xi_1, \ldots, \xi_{N_{\mathrm{bin}}-1}]$ is crucial for ranging error. Consider the N_{bin} hypothesis tests for a given channel instantiation $\boldsymbol{\theta}$

$$\mathcal{H}_{0i} : \mathsf{b}_i \frac{N_{\mathrm{sr}}}{\sigma^2} \overset{|\boldsymbol{\theta}_{\mathrm{b}}}{\sim} \chi^2_{N_{\mathrm{sr}} N_{\mathrm{sb}}}(0) \tag{6a}$$

$$\mathcal{H}_{1i} : \mathsf{b}_i \frac{N_{\mathrm{sr}}}{\sigma^2} \overset{|\boldsymbol{\theta}_{\mathrm{b}}}{\sim} \chi^2_{N_{\mathrm{sr}} N_{\mathrm{sb}}}(\lambda_i \neq 0) \tag{6b}$$

where $i \in \mathcal{B}$, $\mathcal{H}_{0i}$ and $\mathcal{H}_{1i}$ are the hypotheses that the ith bin contains noise only or also the transmitted signal, respectively. The optimal test rejects $\mathcal{H}_{0i}$ with test statistics $\mathsf{b}_i > \xi_i$, and TCS selects the smallest bin index i for which this happens.

A. Constant Threshold Profile

The most common approach in solving the hypothesis testing problem (6) is to set a constant threshold profile (i.e., $\xi_i = \xi_{\mathrm{fa}}\ \forall i \in \mathcal{B}$) such that $P_{\mathrm{fa}}(\boldsymbol{\theta}) = P^{\star}_{\mathrm{fa}}$, where $P^{\star}_{\mathrm{fa}}$ is the maximum tolerable false-alarm probability. Since the false-alarm event occurs in the absence of the signal, the energy

[3] In the terminology of multiple hypothesis tests, the false-alarm probability corresponds to the family-wise error rate [26].

This article has been accepted for publication in a future issue of this journal, but has not been fully edited. Content may change prior to final publication. Citation information: DOI 10.1109/LSP.2018.2815692, IEEE Signal Processing Letters

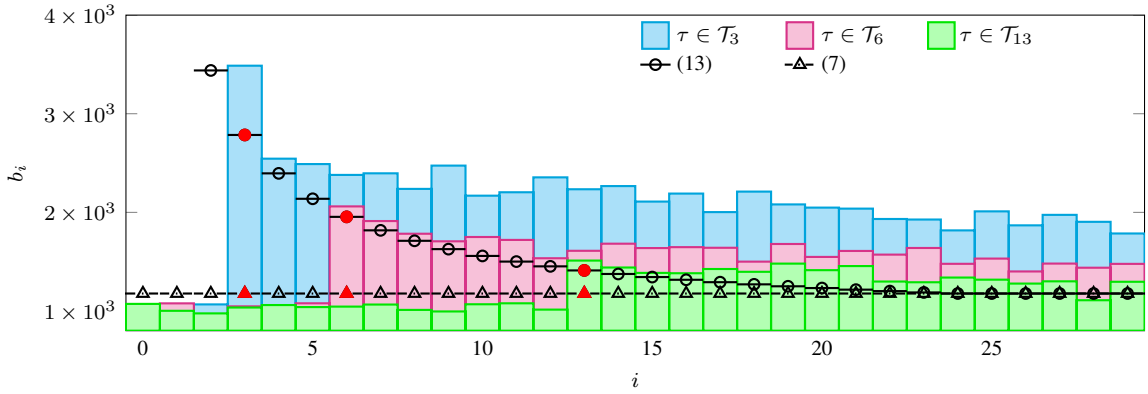

Fig. 2. Example of energy bin vectors and threshold profiling. Each element b_i is an instantiation of the RV b_i. The true bins containing the first signal samples are highlighted with red marks.

bins b_i contain only noise and are independent and identically distributed RVs. From (6a), the threshold $\forall i \in \mathcal{B}$ is

$$\xi_{\text{fa}} = F_{\mathsf{b}_i}^{-1}\Big(\big(1 - P_{\text{fa}}^{\star}\big)^{\frac{1}{N_{\text{bin}}}} \big| \boldsymbol{\theta}_{\text{b}}\Big) . \tag{7}$$

B. Variable Threshold Profile

We propose the use of a variable threshold profile that fulfills a requirement on the ranging error. In particular, the threshold profile is set to guarantee a minimum tolerable value $P_{\text{c}}^{\star}$ for the probability of selecting the correct bin index (i.e., i when $\tau \in \mathcal{T}_i$) to minimize the ranging error.

Lemma 3.1: The probability of selecting the correct bin for $\tau \in \mathcal{T}_i$ is lower bounded by

$$P_{\text{c},i}(\boldsymbol{\theta}_{\text{b}}) \geqslant P_{\text{c}}^{\star} \tag{8}$$

when $\xi_j^{(\text{L})} \leqslant \xi_j \leqslant \xi_j^{(\text{U})}$, $\forall j \in \mathcal{B}$, where

$$\xi_j^{(\text{L})} = \min_{\boldsymbol{\theta}:\lambda_j = 0} F_{\mathsf{b}_j}^{-1}\Big(P_{\text{c}}^{\star\,\frac{1}{N_{\text{bin}}}} \Big| \boldsymbol{\theta}_{\text{b}}\Big) \tag{9a}$$

$$\xi_j^{(\text{U})} = \max_{\boldsymbol{\theta}:\tau \in \mathcal{T}_j} F_{\mathsf{b}_j}^{-1}\Big(1 - P_{\text{c}}^{\star\,\frac{1}{j+1}} \Big| \boldsymbol{\theta}_{\text{b}}\Big) . \tag{9b}$$

Proof: For $\tau \in \mathcal{T}_i$, it is

$$\begin{aligned} &\mathsf{b}_i \frac{N_{\text{sr}}}{\sigma^2} \overset{|\boldsymbol{\theta}_{\text{b}}}{\sim} \chi^2_{N_{\text{sr}}N_{\text{sb}}}(\lambda_i) \text{ with } \lambda_i \neq 0 \\ &\mathsf{b}_j \frac{N_{\text{sr}}}{\sigma^2} \overset{|\boldsymbol{\theta}_{\text{b}}}{\sim} \chi^2_{N_{\text{sr}}N_{\text{sb}}}(0) \ \forall j \in \mathcal{I}_i(i) . \end{aligned} \tag{10}$$

Since $F_{\mathsf{b}_j}(\xi_j)$ is monotonically increasing with ξ_j, if $\xi_j^{(\text{L})} \leqslant \xi_j \leqslant \xi_j^{(\text{U})} \forall j \in \mathcal{B}$, then

$$P_{\text{c},i}(\boldsymbol{\theta}_{\text{b}}) \geqslant \Big[1 - F_{\mathsf{b}_i}(\xi_i^{(\text{U})} | \boldsymbol{\theta}_{\text{b}})\Big] \prod_{j \in \mathcal{I}_i(i)} F_{\mathsf{b}_j}(\xi_j^{(\text{L})} | \boldsymbol{\theta}_{\text{b}}) \tag{11a}$$

$$= P_{\text{c}}^{\star\,\frac{1}{i+1}} P_{\text{c}}^{\star\,\frac{i}{N_{\text{bin}}}} \tag{11b}$$

where the first term in (11b) is from (9b) and the second term is from (9a). As $P_{\text{c}}^{\star} \in [0, 1]$, then for all $i \in \mathcal{B}$ we have

$$P_{\text{c},i}(\boldsymbol{\theta}_{\text{b}}) \geqslant P_{\text{c}}^{\star\,\frac{1}{i+1}} P_{\text{c}}^{\star\,\frac{i}{i+1}} \tag{12}$$

resulting in (8). □

Lemma 3.1 enables the design of a variable threshold profile for fulfilling a requirement on ranging error. An approach that accounts for requirements on both false-alarm probability and ranging error sets the variable threshold profile as

$$\xi_i = \max\left\{\xi_{\text{fa}}, \xi_i^{(\text{U})}\right\} . \tag{13}$$

Then, (13) fulfills both the false-alarm probability requirement and the requirement on ranging error when $\xi_{\text{fa}} \leqslant \xi_i^{(\text{U})}$, $\forall i \in \mathcal{B}$.

Fig. 2 shows some examples of energy bin vectors for three different TOAs. The energy values are compared with the constant (7) and variable (13) threshold profiles with $P_{\text{fa}}^{\star} = 0.01$ and $P_{\text{c}}^{\star} = 0.9$. It can be observed that the variable threshold profile decays with the index of the true bin i. Therefore, the variable threshold is expected to provide a lower false-alarm probability since $\xi_i \geqslant \xi_{\text{fa}}$ $\forall i \in \mathcal{B}$. Moreover, incorrectly selecting a bin is less probable, which is beneficial for reducing early-detection probability (the probability of estimating a smaller TOA than the true one) and ranging error.

Note that (9a) and (9b) require to invert the CDF of the jth bin, which is a non-central chi-square RV. This is a complex operation often performed through numerical evaluations or via approximations. For this reason, a tractable model is necessary for the application of Lemma 3.1 in practical scenarios.

C. Tractable Model for Variable Threshold Profile

The design of variable threshold profile described in Sec. III-B needs to consider the following two aspects: (i) the non-central chi-squared RV does not admit a closed-form CDF expression; and (ii) the instantaneous channel state information $\boldsymbol{\theta}$ is usually not perfectly known. In particular, a tractable model is proposed for the variable threshold profile using an approximation for the CDF of the bin value conditioned on the channel statistics $\overline{\boldsymbol{\theta}}$ instead of the channel instantiation $\boldsymbol{\theta}$. Specifically, we consider the non-centrality parameter as $\lambda_i \simeq \overline{\lambda}_i$, which is deterministic and is calculated from (2) through the average channel parameters $\overline{\boldsymbol{\theta}}$. When λ_i is replaced with $\overline{\lambda}_i$ in (1), the chi-squared RVs can be approximated by Gaussian RVs [25]. In particular, the N_{bin} hypothesis tests in (6) for a given $\overline{\boldsymbol{\theta}}$ become

$$\begin{aligned} \tilde{\mathcal{H}}_{0i} &: \mathsf{b}_i \frac{N_{\text{sr}}}{\sigma^2} \overset{|\overline{\boldsymbol{\theta}}_{\text{b}}}{\sim} \mathcal{N}(N_{\text{sr}}N_{\text{sb}}, 2N_{\text{sr}}N_{\text{sb}}) \\ \tilde{\mathcal{H}}_{1i} &: \mathsf{b}_i \frac{N_{\text{sr}}}{\sigma^2} \overset{|\overline{\boldsymbol{\theta}}_{\text{b}}}{\sim} \mathcal{N}(N_{\text{sr}}N_{\text{sb}} + \overline{\lambda}_i, 2N_{\text{sr}}N_{\text{sb}} + 4\overline{\lambda}_i) . \end{aligned}$$

This article has been accepted for publication in a future issue of this journal, but has not been fully edited. Content may change prior to final publication. Citation information: DOI 10.1109/LSP.2018.2815692, IEEE Signal Processing Letters

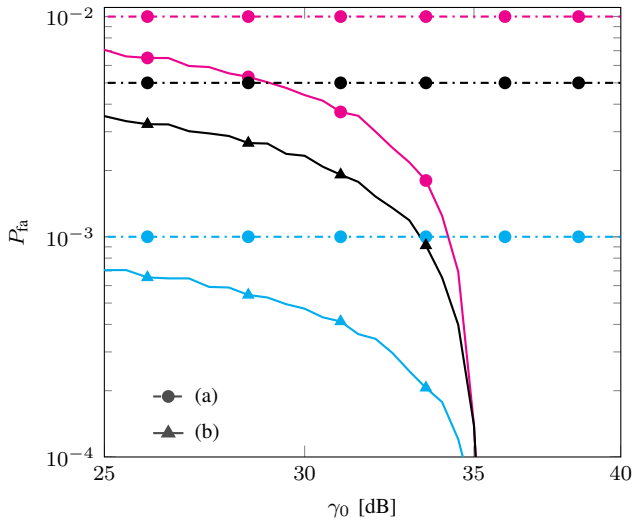

Fig. 3. False-alarm probability as a function of γ_0 for $P_{\text{fa}}^\star = 10^{-2}$ (magenta), $P_{\text{fa}}^\star = 5 \times 10^{-3}$ (cyan), $P_{\text{fa}}^\star = 10^{-3}$ (black) with (a) $\xi_i = \xi_{\text{fa}}$ and (b) $\xi_i = \max\{\xi_{\text{fa}}, \xi_i^{(\text{U})}\}$.

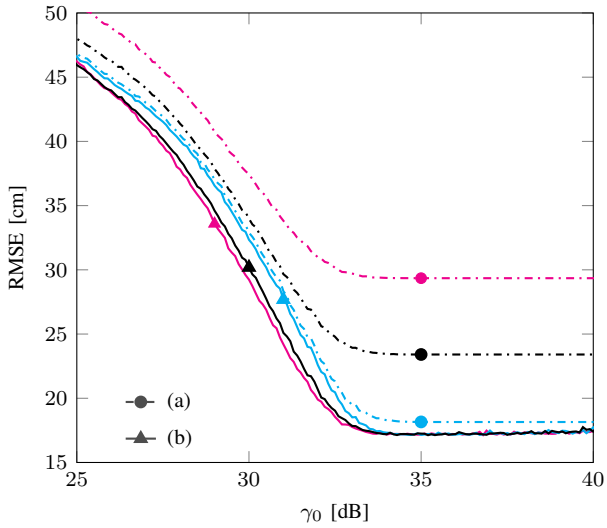

Fig. 4. Root-mean-square of the ranging error as a function of γ_0 for $P_{\text{fa}}^\star = 10^{-2}$ (magenta), $P_{\text{fa}}^\star = 5 \times 10^{-3}$ (cyan), $P_{\text{fa}}^\star = 10^{-3}$ (black) with (a) $\xi_i = \xi_{\text{fa}}$ and (b) $\xi_i = \max\{\xi_{\text{fa}}, \xi_i^{(\text{U})}\}$.

From (9), a closed-form expression for $\xi_i^{(\text{L})}$ and $\xi_i^{(\text{U})}$ is

$$\xi_i^{(\text{L})} \simeq \Phi^{-1}(P_{\text{c}}^{\star\,\frac{1}{N_{\text{bin}}}})\sqrt{2N_{\text{sr}}N_{\text{sb}}} + N_{\text{sr}}N_{\text{sb}}$$

$$\xi_i^{(\text{U})} \simeq \Phi^{-1}(1 - P_{\text{c}}^{\star\,\frac{1}{i+1}})\sqrt{2N_{\text{sr}}N_{\text{sb}} + 4\overline{\lambda}_i} + N_{\text{sr}}N_{\text{sb}} + \overline{\lambda}_i$$

where $\Phi^{-1}(\cdot)$ is the inverse CDF of a standard Gaussian RV.

A further simplification for $\xi_i^{(\text{U})}$ can be made for tapped-delay line channels with exponential power dispersion profile [27]. In such a case, the average non-centrality parameter for the ith bin $\overline{\lambda}_i$ when $\tau \in \mathcal{T}_i$ can be expressed as

$$\overline{\lambda}_i = \overline{\nu}_0 \left(\frac{d_i}{\delta_0}\right)^{-\alpha}$$

where $\overline{\nu}_0$ is the non-centrality parameter corresponding to the correct bin when the first path is related to the reference distance $d = \delta_0$, α is the path-loss exponent, $d_i = g(i)\,c$, and c is the speed of light. The tractable expression for $\xi_i^{(\text{U})}$ is found to be

$$\xi_i^{(\text{U})} = \Phi^{-1}(1 - P_{\text{c}}^{\star\,\frac{1}{i+1}})\sqrt{2N_{\text{sr}}N_{\text{sb}} + 4\overline{\nu}_0 \left(\frac{d_i}{\delta_0}\right)^{-\alpha}} + N_{\text{sr}}N_{\text{sb}} + \overline{\nu}_0 \left(\frac{d_i}{\delta_0}\right)^{-\alpha}. \quad (15)$$

IV. Case Study

The performance improvement of the variable threshold profile is now evaluated using TCS algorithms compared to the constant threshold profile. The energy detector is set with $N_{\text{sr}} = 128$, $T_{\text{obs}} = T_{\text{sr}} = 100\,\text{ns}$, $T_{\text{d}} = 2\,\text{ns}$, and $N_{\text{bin}} = 50$. A tapped-delay line channel is considered, with exponential power dispersion profile and $\alpha = 2.4$ as in [27]. Results are presented for different values of γ_0, which is the SNR at the reference distance $\delta_0 = 1\,\text{m}$. Two different methods for choosing thresholds ξ_i, $\forall i \in \mathcal{B}$, are considered: the constant threshold profile $\xi_i = \xi_{\text{fa}}$; and the variable threshold profile $\xi_i = \max\{\xi_{\text{fa}}, \xi_i^{(\text{U})}\}$ through (15) with $P_{\text{c}}^\star = 0.9$ (i.e., correct bin selected at least 90% of times).

Fig. 3 shows the false-alarm probability as a function of γ_0 for $P_{\text{fa}}^\star = 10^{-3}, 5 \times 10^{-3}$, and 10^{-2}. It can be observed that the false-alarm probability obtained with the variable threshold profile is significantly lower than or equal to that obtained with the constant threshold profile, and it decreases with γ_0.[4]

Fig. 4 shows the root-mean-square of the ranging error $|\hat{\tau} - \tau|$ as a function of γ_0 for $P_{\text{fa}}^\star = 10^{-3}, 5 \times 10^{-3}$, and 10^{-2}, respectively. It can be observed that the variable threshold profile always outperforms the constant threshold profile and the performance gap increases with γ_0 and $P_{\text{fa}}^\star$. The floor value obtained with the variable threshold profile corresponds to the minimum root-mean-square error that is achievable through an energy detector in ideal propagation conditions. In particular, such a floor is $c\,T_{\text{d}}/\sqrt{12} \simeq 17\,\text{cm}$, which is the quantization error due to the temporal resolution of the bin vector.

V. Conclusion

A variable threshold profile for TOA-based ranging was proposed, where the ED threshold design is driven by requirements on both ranging error and false-alarm probability. Tractable expressions for the variable threshold profile were obtained, enabling a simple and yet efficient ranging system design. In particular, the design of the variable threshold profile is based only on statistics rather than instantiations of the wireless channel. A case study for a wideband ranging system showed that the variable threshold profile can significantly improve the performance, compared to conventional methods, in terms of both ranging error and false-alarm probability.

[4] Although not reported in detail for brevity, it was observed that the variable threshold profile improves the false-alarm probability with respect to the constant threshold profile without any degradation of the detection probability.

REFERENCES

[1] M. Z. Win, A. Conti, S. Mazuelas, Y. Shen, W. M. Gifford, D. Dardari, and M. Chiani, "Network localization and navigation via cooperation," *IEEE Commun. Mag.*, vol. 49, no. 5, pp. 56–62, May 2011.

[2] K. Pahlavan, X. Li, and J.-P. Mäkelä, "Indoor geolocation science and technology," *IEEE Commun. Mag.*, vol. 40, no. 2, pp. 112–118, Feb. 2002.

[3] S. Gezici, Z. Tian, G. B. Giannakis, H. Kobayashi, A. F. Molisch, H. V. Poor, and Z. Sahinoglu, "Localization via ultra-wideband radios: A look at positioning aspects for future sensor networks," *IEEE Signal Process. Mag.*, vol. 22, no. 4, pp. 70–84, Jul. 2005.

[4] M. W. M. G. Dissanayake, P. Newman, S. Clark, H. F. Durrant-Whyte, and M. Csorba, "A solution to the simultaneous localization and map building (SLAM) problem," *IEEE Trans. Robot. Autom.*, vol. 17, no. 3, pp. 229–241, Jun. 2001.

[5] G. Cardone, P. Bellavista, A. Corradi, C. Borcea, M. Talasila, and R. Curtmola, "Fostering participaction in smart cities: A geo-social crowdsensing platform," *IEEE Commun. Mag.*, vol. 51, no. 6, pp. 112–119, Jun. 2013.

[6] F. Zabini and A. Conti, "Inhomogeneous Poisson sampling of finite-energy signals with uncertainties in $\mathbb{R}^d$," *IEEE Trans. Signal Process.*, vol. 64, no. 18, pp. 4679–4694, Sep. 2016.

[7] X. Wang, S. Yuan, R. Laur, and W. Lang, "Dynamic localization based on spatial reasoning with RSSI in wireless sensor networks for transport logistics," *Sensors and Actuators A: Physical*, vol. 171, no. 2, pp. 421–428, Nov. 2011.

[8] S. M. George, W. Zhou, H. Chenji, M. Won, Y. O. Lee, A. Pazarloglou, R. Stoleru, and P. Barooah, "Distressnet: A wireless Ad Hoc and sensor network architecture for situation management in disaster response," *IEEE Commun. Mag.*, vol. 48, no. 3, pp. 128–136, Mar. 2010.

[9] D. Dardari, A. Conti, C. Buratti, and R. Verdone, "Mathematical evaluation of environmental monitoring estimation error through energy-efficient wireless sensor networks," *IEEE Trans. Mobile Comput.*, vol. 6, no. 7, pp. 790–802, Jul. 2007.

[10] L. Evans, "Maps as deep: Reading the code of location-based social networks," *IEEE Technol. Soc. Mag.*, vol. 33, no. 1, pp. 73–80, Mar. 2014.

[11] D. Dardari, A. Conti, U. J. Ferner, A. Giorgetti, and M. Z. Win, "Ranging with ultrawide bandwidth signals in multipath environments," *Proc. IEEE*, vol. 97, no. 2, pp. 404–426, Feb. 2009.

[12] L. Lu, H. Zhang, and H.-C. Wu, "Novel energy-based localization technique for multiple sources," *IEEE Syst. J.*, vol. 8, no. 1, pp. 142–150, Mar. 2014.

[13] Y. Shen, S. Mazuelas, and M. Z. Win, "Network navigation: Theory and interpretation," *IEEE J. Sel. Areas Commun.*, vol. 30, no. 9, pp. 1823–1834, Oct. 2012.

[14] H. Urkowitz, "Energy detection for unknown deterministic signal," *Proc. IEEE*, vol. 55, no. 4, pp. 523–531, Apr. 1967.

[15] S. A. Ji, S. J. Lee, and J. S. Kim, "Simplified structure of weighted energy detector for UWB-IR systems," *Electron. Lett.*, vol. 48, no. 1, pp. 48–50, Jan. 2012.

[16] G. Zheng, N. Han, X. Huang, S. H. Sohn, and J. M. Kim, in *Proc. Int. Symp. on Ultra Wideband Sys. and Technol.*, Trondheim, Norway.

[17] B. C. Geiger, T. Gigl, and K. Witrisal, "Enhanced-accuracy channel estimation and ranging for IR-UWB energy detectors," in *Proc. IEEE Int. Conf. on Ultra-Wideband*, Nanjing, China, Sep. 2010, pp. 1–6.

[18] M. I. Skolnik, *Introduction to Radar Systems*, 3rd ed. New York: Mcgraw-Hill, 2002.

[19] J.-Y. Lee and R. A. Scholtz, "Ranging in a dense multipath environment using an UWB radio link," *IEEE J. Sel. Areas Commun.*, vol. 20, no. 9, pp. 1677–1683, Dec. 2002.

[20] R. A. Scholtz and J.-Y. Lee, "Problems in modeling UWB channels," *Electronic letters*, vol. 20, no. 9, pp. 1–10, Dec. 2002.

[21] I. Guvenc and Z. Sahinoglu, "Threshold-based TOA estimation for impulse radio UWB systems," in *Proc. IEEE Int. Conf. on Ultra-Wideband*, Zurich, Switzerland, Sep. 2005, pp. 420–425.

[22] D. Dardari, C.-C. Chong, and M. Z. Win, "Threshold-based time-of-arrival estimators in UWB dense multipath channels," *IEEE Trans. Commun.*, vol. 56, no. 8, pp. 1366–1378, Aug. 2008.

[23] C. Xu and C. L. Law, "Delay-dependent threshold selection for UWB TOA estimation," *IEEE Commun. Lett.*, vol. 12, no. 5, pp. 380–382, May 2008.

[24] F. Guidi, N. Decarli, S. Bartoletti, A. Conti, and D. Dardari, "Detection of multiple tags based on impulsive backscattered signals," *IEEE Trans. Commun.*, vol. 62, no. 11, pp. 3918–3930, Nov. 2014.

[25] S. Bartoletti, W. Dai, A. Conti, and M. Z. Win, "A mathematical model for wideband ranging," *IEEE J. Sel. Topics Signal Process.*, vol. 9, no. 2, pp. 216–228, Mar. 2015.

[26] Y. Hochberg and A. C. Tamhane, *Multiple Comparison Procedures*. New York: Wiley, 1987.

[27] D. Cassioli, M. Z. Win, and A. F. Molisch, "The ultra-wide bandwidth indoor channel: From statistical model to simulations," *IEEE J. Sel. Areas Commun.*, vol. 20, no. 6, pp. 1247–1257, Aug. 2002.